ORIGINAL ARTICLE

European Journal of BREAST HEALTH

DOI: 10.4274/ejbh.galenos.2026.2026-1-9
Eur J Breast Health 2026;22(3):350-357

Interim Breast MRI for Predicting Pathologic Complete Response After Neoadjuvant Chemotherapy in Early Breast Cancer

Eri Kato[1], Hideo Shigematsu[1], Ai Amioka[1], Shinsuke Sasada[1], Takayuki Kadoya[1,2], Morihito Okada[1]

[1]Department of Surgical Oncology, Hiroshima University, Research Institute for Radiation Biology and Medicine, Hiroshima, Japan
[2]Department of Breast Center, Shimane University Hospital, Izumo, Japan

ABSTRACT

Objective: Accurate prediction of pathological complete response (pCR) to neoadjuvant chemotherapy (NAC) is essential for treatment decision-making in breast cancer. The value of integrated prediction models combining interim magnetic resonance imaging (MRI) findings with clinicopathological factors remains uncertain. This study aimed to compare interim and post-NAC MRI in predicting pCR and to assess the performance of prediction models integrating MRI and clinicopathological variables.

Materials and Methods: We retrospectively analyzed 249 patients with early-stage breast cancer who underwent MRI before, during (interim), and after NAC. Clinicopathological variables were selected via stepwise regression based on the minimum Akaike information criterion. Four predictive models were developed: Model A used clinicopathological variables alone; Model B added interim MRI; Model C added post-NAC MRI; and Model D incorporated both interim and post-NAC MRI. Model performance was assessed using receiver operating characteristic curve analysis, calibration plots, and decision curve analysis.

Results: Sixty-two (25%) patients achieved pCR. Independent predictors in Model A included hormone receptor status, human epidermal growth factor receptor 2 status, and clinical tumor size. The areas under the curves were 0.721 (Model A), 0.819 (Model B), 0.847 (Model C), and 0.848 (Model D). Model B (interim MRI) demonstrated the highest sensitivity (0.99) and negative predictive value (0.97), enabling early identification of pCR, while Models C and D showed only modest improvements. In decision curve analysis, calibration and clinical utility were superior in models incorporating MRI compared with Model A.

Conclusion: Interim MRI demonstrated pCR-predictive performance comparable to that of post-NAC MRI, supporting its potential utility as a clinically meaningful tool for early treatment decision-making. However, its relatively high false-positive rate suggests that caution is warranted when applying it to guide surgical de-escalation.

Keywords: Breast neoplasms; neoadjuvant therapy; magnetic resonance imaging; pathologic complete response; predictive value of tests

Corresponding Author: Hideo Shigematsu, MD, PhD;
E-mail: shigematu1330@hiroshima-u.ac.jp **ORCID:** orcid.org/0000-0001-9393-9655
Received: 10.02.2026 **Accepted:** 19.05.2026 **Available Online Date:** 17.06.2026
Cite this article as: Kato E, Shigematsu H, Amioka A, Sasada S, Kadoya T, Okada M. Interim breast MRI for predicting pathologic complete response after neoadjuvant chemotherapy in early breast cancer. Eur J Breast Health. 2026;22(3):350-357

KEY POINTS

- Interim magnetic resonance imaging (MRI), performed during neoadjuvant chemotherapy (NAC) treatment, demonstrated significant predictive ability for post-NAC pathological complete response (pCR) in patients with breast cancer.
- Combining interim MRI findings with clinicopathological factors improved predictive accuracy for pCR.
- Interim MRI may contribute to early identification of non-responders and support treatment decision-making.
- This study provides real-world evidence supporting the clinical utility of interim MRI in patients with breast cancer undergoing NAC.

Introduction

Although surgery-first has traditionally been the standard approach in early-stage breast cancer, neoadjuvant chemotherapy (NAC) is increasingly used and represents a standard treatment option in selected subtypes, particularly human epidermal growth factor receptor 2 (HER2)-positive and triple-negative breast cancer, in the context of surgical de-escalation and response-guided therapy (1). With advances in systemic therapy, treatment response rates have improved, and the number of patients achieving pathological complete response (pCR) has increased. With these improvements, clinical trials investigating the omission of surgery in responders are underway, but the development of surgical de-escalation strategies requires accurate and less invasive identification of pCR in patients with breast cancer undergoing NAC (2).

Among imaging modalities used to assess response to NAC, contrast-enhanced magnetic resonance imaging (MRI) is considered to be the most reliable technique (3). However, MRI alone has limited accuracy in predicting pCR, and its diagnostic performance varies according to breast cancer subtype, with lower accuracy reported in hormone receptor (HR)-positive/HER2-negative breast cancer and higher accuracy in HER2-positive and triple-negative subtypes (3, 4). To address these limitations, several integrated prediction models that combine MRI features with clinicopathological variables (e.g., tumor size, HR status, HER2 status, and Ki-67 index) have been proposed, demonstrating superior and less invasive pCR prediction compared with MRI alone (5, 6).

Recent studies have further suggested that pCR may be predicted more accurately based on MRI performed during NAC treatment (interim MRI) than on post-NAC MRI (7). Quantitative longitudinal parameters, such as changes in tumor size, apparent diffusion coefficient values on diffusion-weighted imaging, and background parenchymal enhancement, have also shown promise in detecting early treatment response (8-10). Nevertheless, studies comparing the diagnostic accuracy of interim and post-NAC MRI or evaluating the clinical utility of integrated prediction models that incorporate clinicopathological variables remain limited (6, 11). Moreover, previous studies defined pCR as the absence of residual invasive cancer in the breast, whereas only a few have adopted the stricter criterion of no residual invasive or non-invasive carcinoma in either the breast or lymph nodes (ypT0, ypN0) (6, 8, 11, 12).

Therefore, we conducted a retrospective cohort study of patients with early-stage breast cancer who underwent MRI during and after NAC. The aim of this study was to compare the predictive performance of interim and post-NAC MRI in predicting pCR (defined as ypT0, ypN0) and to evaluate the diagnostic performance and clinical usefulness of integrated prediction models combining MRI findings with clinicopathological factors.

Materials and Methods

Study Design and Patients

This single-center, retrospective, observational study was conducted at Hiroshima University Hospital using data derived from a multicenter database; however, only patients treated at our institution were included in the present analysis. This is because interim MRI was not routinely performed at all participating institutions, and including data from multiple centers would have resulted in substantial heterogeneity and potentially missing data in MRI assessments. To ensure consistency and completeness of imaging data and uniformity in clinical management and MRI interpretation, we limited the analysis to a single-center cohort. The study included patients with breast cancer who underwent NAC between April 2010 and December 2020. All women with invasive breast cancer were eligible if they underwent MRI at three time points: before NAC, during the early phase of treatment (interim MRI, i.e., after completion of the first half of chemotherapy), and after completion of NAC (post-NAC MRI). Both imaging and pathological evaluation data were required for patient inclusion.

The exclusion criteria were as follows: (1) presence of distant metastasis; (2) discontinuation of NAC before completion; and (3) absence of MRI or insufficient image quality for evaluation at any of the three time points. Clinical data were obtained from electronic medical records and the picture archiving and communication system.

This study was approved by the Ethics Committee for Epidemiology of Hiroshima University (approval number: E2014-

1157-06, date: 25.07.2023) and was conducted in accordance with the Declaration of Helsinki. Formal patient consent was not required for this retrospective study.

Clinicopathological Factors

The candidate predictors for pCR included clinical tumor size (T category), clinical nodal status (N category), HR status, HER2 expression, and nuclear grade. T and N categories were determined according to the 8th edition of the American Joint Committee on Cancer TNM staging system based on tumor size and clinical nodal status (13).

HR-positivity was defined as positive staining for either the estrogen receptor (ER) or the progesterone receptor. Tumors with ≥1% positively stained tumor cells on immunohistochemistry (IHC) were considered HR-positive. HER2 status was determined in accordance with the American Society of Clinical Oncology/College of American Pathologists guidelines and was defined as positive if scored as IHC 3+ or confirmed as amplified by fluorescence *in situ* hybridization (14, 15). All clinicopathological assessments were based on needle biopsy specimens and imaging findings obtained before initiation of NAC. pCR was defined as no residual invasive or non-invasive carcinoma in both the breast and axillary lymph nodes (ypT0, ypN0).

NAC Regimen

NAC was administered according to standard institutional protocols consisting of sequential anthracycline- and taxane-based chemotherapy regimens. Dose-dense schedules were also adopted in selected cases. For patients with HER2-positive breast cancer, trastuzumab was administered concurrently with taxanes. Pertuzumab was additionally incorporated after its approval for early breast cancer in 2013 (16).

MRI Acquisition and Evaluation

Breast MRI examinations were performed using a 1.5-Tesla scanner (Achieva; Philips Healthcare, Best, the Netherlands) with a dedicated breast coil. A gadolinium-based contrast agent (0.1 mmol/kg) was administered intravenously at a rate of 2.0 mL/s using a bolus injection, followed by a saline flush of at least 10 mL.

The imaging protocol included axial diffusion-weighted imaging (b-value: 1500 s/mm^2), axial T1-weighted imaging, axial fat-suppressed T2-weighted imaging, and dynamic contrast-enhanced, fat-suppressed T1-weighted imaging using a 3D turbo field echo sequence (e-THRIVE). Dynamic images were acquired at 0, 1, 2, and 5 minutes after contrast administration. Additional sagittal contrast-enhanced T1-weighted images were acquired separately for each breast.

The slice thickness ranged from 1.6 to 5.0 mm depending on the sequence, and fat suppression was performed using SPAIR. MRI was performed at three time points: before NAC, during NAC, and after NAC.

MRI assessments were based on final radiological reports, documented by board-certified radiologists in the electronic medical records. MRI examinations were interpreted under a double-reading system by two board-certified radiologists. All radiologists had experience in breast MRI interpretation. MRI examinations were interpreted with access to clinical information, including the treatment course, as part of routine clinical practice. The readers were not fully blinded to pathological outcomes owing to the retrospective design of the study. Using information on the presence or absence of residual lesions and on the degree of contrast enhancement described in the reports, the investigators determined the final MRI findings for this study. Radiologic complete response (rCR) was defined as the complete disappearance of contrast enhancement at the tumor site on contrast-enhanced MRI.

Statistical Analysis

Logistic regression models were constructed with pCR (ypT0, ypN0) as the dependent variable. First, Model A was developed using only clinicopathological variables, without MRI findings. Variable selection was performed using a stepwise method based on the minimum Akaike information criterion (AIC). The assessments of rCR on interim and post-NAC MRI were sequentially added to the clinicopathological factors to construct Models B and C, respectively. Model D included both interim and post-NAC MRI assessments to evaluate their combined predictive value.

Model performance was compared using the area under the receiver operating characteristic (ROC) curve (AUC) as the primary metric. Internal validation was performed using bootstrap resampling with 1,000 iterations to assess model discrimination. Sensitivity and specificity were also calculated to evaluate discriminative ability. To assess clinical usefulness, decision curve analysis was conducted to compare net benefits across a range of threshold probabilities.

All statistical analyses were performed using R statistical software (version 4.5.0; the R foundation for statistical computing, Vienna, Austria). A two-sided p-value <0.05 was considered statistically significant. There were no missing data for the variables included in the regression analysis. Analyses were performed by breast cancer subtype (HR-positive/HER2-negative, HER2-positive, and triple-negative). Diagnostic performance metrics, including sensitivity, specificity, positive predictive value (PPV), and negative predictive value (NPV), were evaluated within each subtype.

Comparison of Diagnostic Performance Metrics

Diagnostic performance of each prediction model was evaluated using sensitivity, specificity, PPV, NPV, false-positive rate (FPR), and overall accuracy. All metrics were calculated to assess the ability of each model to predict pCR.

Sensitivity was defined as the proportion of patients with pCR correctly identified by the model. Specificity was defined as the proportion of patients without pCR who were correctly predicted as not having pCR. PPV and NPV were calculated from the counts of true-positive, true-negative, false-positive, and false-negative cases. FPR was defined as the proportion of patients without pCR who were incorrectly predicted to have pCR (1-specificity), and accuracy the proportion of correctly classified cases among all patients.

Results

Patient Characteristics

A total of 249 patients with invasive breast cancer were included in the analysis. The median age was 52 years. Clinical T1–2 tumors were present in 195 (78%) patients, and 133 (53%) had clinically positive lymph nodes. pCR was observed in 62 patients (25%; Table 1).

Logistic Regression Analysis of Clinicopathological Predictors of pCR

Multivariable logistic regression analysis identified three independent predictors associated with pCR for Model A: HR status, HER2 expression, and clinical T category. Clinical T category ≥3 [odds ratio (OR) 0.32; 95% confidence interval (CI) 0.10–0.79; $p = 0.023$] and HR-positivity (OR 0.42; 95% CI 0.22–0.80; $p = 0.008$) were significantly associated with non-pCR, whereas HER2-positivity (OR 2.38; 95% CI 1.27–4.51; $p = 0.007$) was significantly associated with pCR. Nuclear grade 3 showed a trend toward significance (OR 1.97; 95% CI 0.98–4.14; $p = 0.063$). The overall model remained statistically significant (likelihood ratio test, $p<0.001$; Table 2).

ROC Analysis and Comparison of Models' Diagnostic Performance

ROC curve analysis showed that the AUCs were 0.721 (95% CI 0.661–0.796) for Model A, 0.819 (95% CI 0.752–0.881) for Model B, 0.847 (95% CI 0.791–0.903) for Model C, and 0.848 (95% CI 0.791–0.906) for Model D. Compared with Model A, all MRI-based models (Models B-D) showed significantly improved discrimination (DeLong test, $p<0.0001$). However, no significant differences were observed among Models B-D ($p = 0.23$–0.95; Figure 1). Bootstrap resampling yielded a mean AUC of 0.829 (95% CI, 0.762–0.891) for Model B, indicating stable model discrimination.

Table 1. Baseline characteristics of the study population ($n = 249$)

Characteristic	*n* (%)
Age (y), median (range)	52 (22–76)
Menopausal status	
Premenopausal	129 (52%)
Postmenopausal	106 **(43%)**
Unknown	**14 (5%)**
Clinical T stage	
T1/T2	195 (78%)
T3/T4	54 (22%)
Clinical N stage	
N-negative	116 (47%)
N-positive	133 (53%)
HR status	
Positive	112 (45%)
HER2 status	
Positive	79 (32%)
Nuclear grade	
Grade 1/2	88 (35%)
Grade 3	161 (65%)
pCR	
Achieved	62 (25%)
Not achieved	187 (75%)
Surgery	
Breast-conserving surgery	91 (37%)
Mastectomy	157 (63%)
Axillary surgery	
Sentinel node biopsy only	104 (42%)
Axillary dissection	144 (58%)

HER2: Human epidermal growth factor receptor 2; HR: Hormone receptor; pCR: Pathological complete response

Table 2. Clinicopathological factors associated with pathological complete response selected by AIC-based stepwise logistic regression (Model A)

Variables	Odds ratio	95% CI	*p*-value
T3 or higher (*vs.* T1–2)	0.32	0.10–0.79	0.023
HR-positive (*vs.* HR-negative)	0.42	0.22–0.80	0.008
HER2-positive (*vs.* HER2-negative)	2.38	1.27–4.51	0.007
Nuclear grade 3 (*vs.* nuclear grade 1–2)	1.97	0.98–4.14	0.063

AIC = 259.19; Pseudo-R^2 = 0.108 (McFadden's R^2). Overall significance of the logistic regression model (likelihood ratio test): $p = 0.0000084$. CI: Confidence interval; AIC: Akaike information criterion; HER2: Human epidermal growth factor receptor 2; HR: Hormone receptor

Calibration

Calibration curve analysis demonstrated that Models B, C, and D, which incorporated MRI information, had better agreement between predicted and observed probabilities than Model A (Figure 2). Model B exhibited good calibration in the low-to-intermediate probability range, whereas Model C tended to slightly underestimate predicted probabilities in the higher-probability range. Model D demonstrated the most consistently favorable calibration across the full range of predicted probabilities.

Clinical Utility based on Decision Curve Analysis

All prediction models demonstrated greater net benefit than did the treat-all and treat-none strategies. Model B provided the greatest net benefit in the higher threshold probability range (≥0.6), whereas Model C showed relatively higher clinical utility in the lower threshold probability range (≤0.3; Figure 3).

Comparison of Diagnostic Accuracy Metrics

Model B demonstrated the highest sensitivity (0.99) and NPV (0.97), indicating an excellent ability to identify patients who achieve pCR. However, Model B also showed the lowest specificity (0.45) and the highest FPR (0.55), suggesting a substantial risk of misclassifying non-pCR cases as pCR.

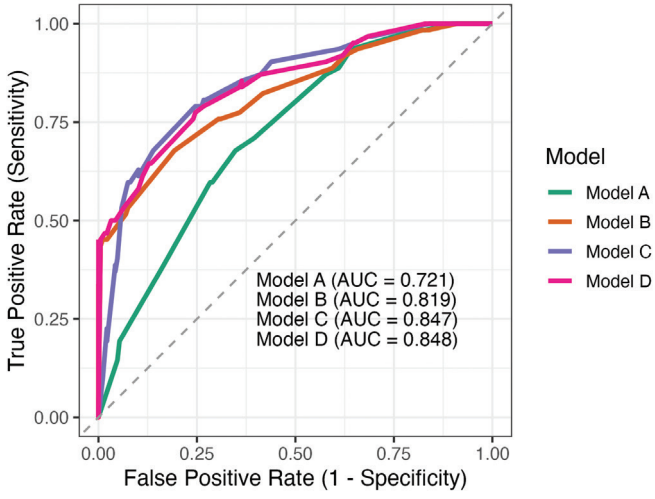

Figure 1. ROC curves of four logistic regression models for predicting pCR. The AUC values were 0.721 for Model A, 0.819 for Model B, 0.847 for Model C, and 0.848 for Model D. Models incorporating MRI information (Models B-D) demonstrated markedly better predictive performance than that of Model A, whereas differences among the MRI-based models were minimal

ROC: Receiver operating characteristic; MRI: Magnetic resonance imaging; pCR: Pathological complete response; AUC: Area under the curve

Model A showed the highest specificity (0.73) and the lowest FPR (0.27). Model C yielded the highest PPV (0.88), while Models C and D demonstrated comparable overall accuracy (0.83), slightly lower than that of Model B (0.86).

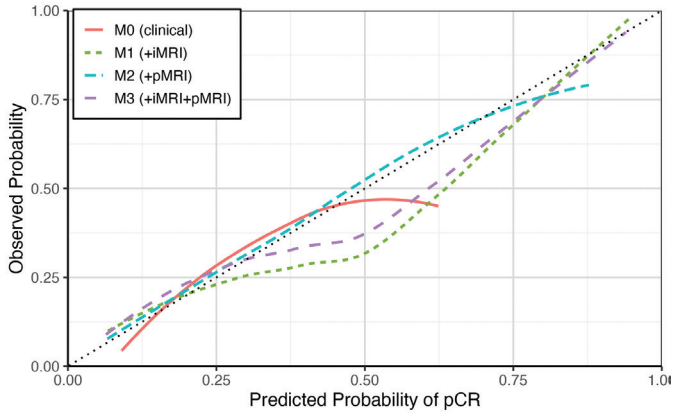

Figure 2. Calibration curves of four prediction models for pCR. Models incorporating MRI information (Models B-D) showed better agreement between predicted and observed probabilities than did Model A, with Model D demonstrating the most consistent calibration across a wide range of predicted probabilities

MRI: Magnetic resonance imaging; pCR: Pathological complete response

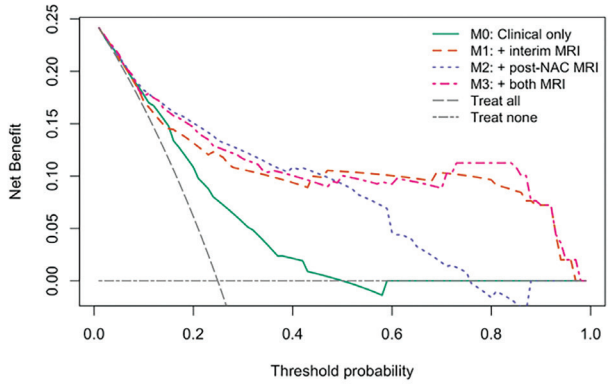

Figure 3. Decision curve analysis of four logistic regression models for predicting pCR. Decision curve analysis of the four prediction models: The vertical axis indicates net benefit, and the horizontal axis indicates the threshold probability for pCR. All models provided greater net benefit than did the treat-all and treat-none strategies. Model B showed the highest clinical utility in the higher threshold probability range (≥0.6), whereas Model C showed relatively greater utility in the lower threshold probability range (≤0.3)

pCR: Pathological complete response; NAC: Neoadjuvant chemotherapy; MRI: Magnetic resonance imaging

These findings indicate that although Model B is highly sensitive and useful for identifying responders, its high FPR may limit its applicability for safely guiding surgical de-escalation (Table 3).

Subtype-Specific Analysis

Subtype-specific analyses revealed differences in diagnostic performance among the models across breast cancer subtypes (HR-positive/HER2-negative, HER2-positive, and triple-negative breast cancer).

Model B showed higher specificity in subtype analyses and lower FPRs across subtypes, whereas Models C and D showed more balanced performance with higher sensitivity. These subtype-specific results are presented in Supplementary Tables 1A-C.

Discussion and Conclusion

In this study, the interim MRI-based pCR prediction model demonstrated a diagnostic performance comparable to that of post-NAC MRI, indicating its potential usefulness for clinical decision-making at an early-stage of treatment. Although Model B achieved the highest sensitivity (0.99) and NPV (0.97), this benefit was associated with the highest FPR (0.55), raising concerns about the risk of overtreatment when applied to surgical de-escalation. Models C and D demonstrated slightly superior overall discrimination with the highest AUC values (0.847 and 0.848); however, the improvement over Model B was marginal, and their FPRs remained moderately high.

Calibration curve analysis showed that MRI-integrated models provided better agreement between predicted and observed probabilities than did Model A, with Model D demonstrating the most stable calibration across all ranges. Decision curve analysis indicated that Model B provided the greatest net benefit at higher threshold probabilities (≥0.6), supporting its value when prioritizing pCR detection for early treatment intensification. Conversely, Model C was more beneficial at lower thresholds (≤0.3), suggesting that these models may have complementary roles depending on specific clinical goals. Taken together, interim MRI offers clinically meaningful predictive performance comparable to that of post-NAC MRI while enabling earlier therapeutic intervention. However, the relatively high FPR indicates that interim MRI alone may not be a safe guide for surgical de-escalation and that integration with post-NAC MRI remains essential to reduce unnecessary undertreatment and to optimize individualized patient care.

Previous prospective studies have also suggested the value of interim MRI for early assessment of treatment response. However, many of these studies were limited by small sample sizes or focused on specific molecular subtypes (e.g., ER-positive/HER2-negative), which may have restricted generalizability to real-world practice (8, 12). In contrast, the present study included all molecular subtypes and incorporated diverse treatment sequences reflective of contemporary clinical practice. Thus, our results provide evidence that the utility of interim MRI can be extrapolated to a broader patient population.

Response-adapted treatment strategies guided by MRI have recently gained attention in NAC. For example, the TRAIN-3 trial evaluated an MRI-guided early termination strategy based on rCR, demonstrating reduced treatment burden without compromising pCR rates (17). The I-SPY 2 trial incorporated early MRI response into its adaptive trial design, reporting a strong association between interim MRI response and pCR (18). These findings highlight the role of interim MRI not only as a predictive imaging biomarker but also as a key component in optimizing treatment duration and regimen selection. Our study supports this concept by demonstrating that combining interim MRI findings with clinicopathological factors can facilitate effective response-adapted clinical decision-making.

The strengths of this study include (1) a relatively large, single-institution cohort of 249 patients; (2) MRI evaluation at three standardized time points (pre-NAC, interim, and post-NAC), covering a broad range of molecular subtypes and treatment regimens reflecting real-world practice; (3) use of a strict definition of pCR (ypT0, ypN0); and (4) comprehensive evaluation

Table 3. Diagnostic performance for predicting pathological complete response in each prediction model

Parameter	Model A	Model B	Model C	Model D
Sensitivity	0.59 (0.52–0.66)	0.99 (0.97–1.00)	0.90 (0.85–0.94)	0.91 (0.86–0.95)
Specificity	0.73 (0.60–0.83)	0.45 (0.32–0.58)	0.63 (0.50–0.75)	0.60 (0.46–0.72)
PPV	0.87 (0.80–0.92)	0.85 (0.79–0.89)	0.88 (0.82–0.92)	0.87 (0.82–0.92)
NPV	0.37 (0.29–0.46)	0.97 (0.82–1.00)	0.67 (0.54–0.79)	0.69 (0.54–0.80)
FPR	0.27 (0.17–0.40)	0.55 (0.42–0.68)	0.37 (0.25–0.50)	0.40 (0.28–0.54)
Accuracy	0.63 (0.56–0.69)	0.86 (0.81–0.90)	0.83 (0.78–0.88)	0.83 (0.78–0.88)

Values are shown as estimates with 95% confidence intervals in parentheses.

FPR: False-positive rate (1-specificity); NPV: Negative predictive value; PPV: Positive predictive value

of discrimination, calibration, and clinical usefulness using decision curve analysis. These features reinforce the clinical applicability of the developed prediction models.

Some limitations should also be acknowledged. First, as this was a single-center retrospective study, potential selection and information biases cannot be excluded. Second, patients were treated between 2010 and 2020, and updated analyses incorporating more recent standard-of-care regimens, including immunotherapy for triple-negative breast cancer, are warranted (19). Third, variable selection was performed using an AIC-based stepwise procedure, which may have introduced data-driven selection bias and potential overfitting. However, internal validation using bootstrap resampling suggested that the model performance was relatively stable, although external validation is warranted.

Fourth, subgroup analyses by breast cancer subtype were performed; however, the results should be interpreted with caution due to the limited sample size in each subgroup. This study did not assess the absolute clinical consequences of false positives (undertreatment) or true positives (benefit), as the primary objective was to compare relative usefulness among models. Future investigations should incorporate regimen-specific toxicity and patient preferences when defining clinically meaningful decision thresholds.

Future Perspectives

External validation using independent cohorts is necessary to confirm the generalizability of our findings. Standardization of MRI acquisition and interpretation criteria should also be pursued. Additionally, incorporating quantitative MRI-derived parameters (e.g., volumetric tumor shrinkage, signal intensity changes) may further improve objectivity and reproducibility in prediction models (20). Ultimately, integration of these predictive models into routine clinical workflows to guide response-adapted strategies and to dynamically optimize treatment duration and regimens based on interim MRI responses will be essential. Such an approach may enhance personalized breast cancer care by maximizing therapeutic benefit while minimizing unnecessary treatment-related toxicities.

In this study, we showed that interim MRI demonstrated predictive performance for pCR in patients with breast cancer that was comparable to that of post-NAC MRI and enabled earlier clinical decision-making, indicating its potential utility as a decision-support tool that can be implemented early in the management of breast cancer.

Ethics

Ethics Committee Approval: This study was approved by the Ethics Committee for Epidemiology of Hiroshima University (approval number: E2014-1157-06, date: 25.07.2023) and was conducted in accordance with the Declaration of Helsinki.

Informed Consent: Formal patient consent was not required for this retrospective study.

Acknowledgements

We would like to thank Dr. Naoyuki Kitamura and Mr. Eikoh Ueda for their valuable support in providing detailed information on MRI acquisition protocols and imaging procedures.

Footnotes

Authorship Contributions

Surgical and Medical Practices: E.K., H.S., A.A., S.S., T.K.; Concept: E.K., H.S., A.A., S.S., T.K., M.O.; Design: E.K., H.S., A.A., S.S., T.K., M.O.; Data Collection and/or Processing: E.K., H.S., A.A., S.S., T.K.; Analysis and/or Interpretation: E.K., H.S.; Literature Search: E.K., H.S.; Writing: E.K., H.S.

Conflict of Interest: The authors have no conflicts of interest to declare.

Financial Disclosure: The authors declared that this study has received no financial support.

Supplementary Tables Link: https://d2v96fxpocvxx.cloudfront.net/e1c28131-4444-460a-9703-9fa751c405df/content-images/ecdea770-ab1b-4d99-a7fe-7248d779e1fc.pdf

References

1. Loibl S, André F, Bachelot T, Barrios CH, Bergh J, Burstein HJ, et al. Early breast cancer: ESMO Clinical Practice Guideline for diagnosis, treatment and follow-up. Ann Oncol. 2024; 35: 159-182. (PMID: 38101773) [Crossref]
2. Johnson HM, Lin H, Shen Y, Diego EJ, Krishnamurthy S, Yang WT, et al. Patient-reported outcomes of omission of breast surgery following neoadjuvant systemic therapy: a nonrandomized clinical trial. JAMA Netw Open. 2023; 6: e2333933. (PMID: 37707811) [Crossref]
3. Janssen LM, den Dekker BM, Gilhuijs KGA, van Diest PJ, van der Wall E, Elias SG. MRI to assess response after neoadjuvant chemotherapy in breast cancer subtypes: a systematic review and meta-analysis. NPJ Breast Cancer. 2022; 8: 107. (PMID: 36123365) [Crossref]
4. Marinovich ML, Houssami N, Macaskill P, Sardanelli F, Irwig L, Mamounas EP, et al. Meta-analysis of magnetic resonance imaging in detecting residual breast cancer after neoadjuvant therapy. J Natl Cancer Inst. 2013; 105: 321-333. (PMID: 23297042) [Crossref]
5. Zhang Y, Cai J, Cui C, Qi S, Zhao D. Predicting breast cancer response to neoadjuvant therapy by integrating radiomic and deep-learning features from early-and-peak phases of DCE-MRI. BMC Cancer. 2025; 25: 1747. (PMID: 41219899) [Crossref]
6. Hajri R, Aboudaram C, Lassau N, Assi T, Antoun L, Ribeiro JM, et al. Prediction of breast cancer response to neoadjuvant therapy with machine learning: a clinical, MRI-qualitative, and radiomics approach. Life (Basel). 2025; 15: 1165. (PMID: 40868813) [Crossref]
7. Fangberget A, Nilsen LB, Hole KH, Holmen MM, Engebraaten O, Naume B, et al. Neoadjuvant chemotherapy in breast cancer—response evaluation and prediction of response to treatment using dynamic contrast-enhanced and

diffusion-weighted MR imaging. Eur Radiol. 2011; 21: 1188-1199. (PMID: 21127880) [Crossref]

8. Hylton NM, Blume JD, Bernreuter WK, Pisano ED, Rosen MA, Morris EA, et al. Locally advanced breast cancer: MR imaging for prediction of response to neoadjuvant chemotherapy—results from ACRIN 6657/I-SPY TRIAL. Radiology. 2012; 263: 663-672. (PMID: 22623692) [Crossref]

9. Suo S, Yin Y, Geng X, Zhang D, Hua J, Cheng F, et al. Diffusion-weighted MRI for predicting pathologic response to neoadjuvant chemotherapy in breast cancer: evaluation with mono-, bi-, and stretched-exponential models. J Transl Med. 2021; 19: 236. (PMID: 34078388) [Crossref]

10. You C, Peng W, Zhi W, He M, Liu G, Xie L, et al. Association between background parenchymal enhancement and pathologic complete remission throughout neoadjuvant chemotherapy in breast cancer patients. Transl Oncol. 2017; 10: 786-792. (PMID: 28806712) [Crossref]

11. Henderson SA, Muhammad Gowdh N, Purdie CA, Jordan LB, Evans A, Brunton T, et al. Breast cancer: influence of tumour volume estimation method at MRI on prediction of pathological response to neoadjuvant chemotherapy. Br J Radiol. 2018; 91: 20180123. (PMID: 29641224) [Crossref]

12. Rigter LS, Loo CE, Linn SC, Sonke GS, van Werkhoven E, Lips EH, et al. Neoadjuvant chemotherapy adaptation and serial MRI response monitoring in ER-positive HER2-negative breast cancer. Br J Cancer. 2013; 109: 2965-2972. (PMID: 24149178) [Crossref]

13. Giuliano AE, Edge SB, Hortobagyi GN. Eighth edition of the AJCC cancer staging manual: breast cancer. Ann Surg Oncol. 2018; 25: 1783-1785. (PMID: 29671136) [Crossref]

14. Allison KH, Hammond MEH, Dowsett M, McKernin SE, Carey LA, Fitzgibbons PL, et al. Estrogen and progesterone receptor testing in breast cancer: American Society of Clinical Oncology/College of American Pathologists Guideline update. Arch Pathol Lab Med. 2020; 144: 545-563. (PMID: 31928354) [Crossref]

15. Wolff AC, Hammond MEH, Allison KH, Harvey BE, McShane LM, Dowsett M. HER2 testing in breast cancer: American Society of Clinical Oncology/College of American Pathologists Clinical Practice Guideline focused update summary. J Oncol Pract. 2018; 14: 437-441. (PMID: 29920138) [Crossref]

16. Gianni L, Pienkowski T, Im YH, Roman L, Tseng LM, Liu MC, et al. Efficacy and safety of neoadjuvant pertuzumab and trastuzumab in women with locally advanced, inflammatory, or early HER2-positive breast cancer (NeoSphere): a randomised multicentre, open-label, phase 2 trial. Lancet Oncol. 2012; 13: 25-32. (PMID: 22153890) [Crossref]

17. van der Voort A, Louis FM, van Ramshorst MS, Kessels R, Mandjes IA, Kemper I, et al. MRI-guided optimisation of neoadjuvant chemotherapy duration in stage II–III HER2-positive breast cancer (TRAIN-3): a multicentre, single-arm, phase 2 study. Lancet Oncol. 2024; 25: 603-613. (PMID: 38588682) [Crossref]

18. Li W, Newitt DC, Wilmes LJ, Jones EF, Arasu V, Gibbs J, et al. Additive value of diffusion-weighted MRI in the I-SPY 2 TRIAL. J Magn Reson Imaging. 2019; 50: 1742-1753. (PMID: 31026118) [Crossref]

19. Schmid P, Cortes J, Dent R, McArthur H, Pusztai L, Kümmel S, et al. KEYNOTE-522 investigators. overall survival with pembrolizumab in early-stage triple-negative breast cancer. N Engl J Med. 2024; 391: 1981-1991. (PMID: 39282906) [Crossref]

20. Tang W, Jin C, Kong Q, Liu C, Chen S, Ding S, et al. Development and validation of an MRI spatiotemporal interaction model for early noninvasive prediction of neoadjuvant chemotherapy response in breast cancer: a multicentre study. EClinicalMedicine. 2025; 85: 103298. (PMID: 40584836) [Crossref]